



Removal of toxic Cr(VI) from water by a novel magnetic chitosan/glyoxal/PVA hydrogel film

Merriam Mirabedini, M.Z. Kassaei*

Department of Chemistry, College of Basic Sciences, Tarbiat Modares University, Tehran, Iran, Tel. +98 9121000392; Fax: +98 2188009730; email: m.mirabedini69@gmail.com (M. Mirabedini), kassaeem@modares.ac.ir (M.Z. Kassaei)

Received 8 October 2014; Accepted 7 June 2015

ABSTRACT

Coprecipitation of FeCl₂ and FeCl₃ produced magnetic iron nanoparticles (Fe₃O₄NPs). The latter was dispersed in an acetic acid solution of chitosan (CS), and then cross-linked with glyoxal, followed by addition of polyvinyl alcohol (PVA). The resulting gel was neutralized with NaOH giving our novel Fe₃O₄NPs/CS/glyoxal/PVA hydrogel film. This film was used as an efficient and reusable adsorbent for the removal of toxic Cr(VI) from water, at a rather wide range of pH. The adsorbent film was characterized by X-ray diffraction, scanning electron microscopy, Fourier transform infrared, and energy dispersive X-ray. Langmuir isotherm model suggested maximum Cr(VI) adsorption occurring at room temperature. Kinetic studies suggested a *pseudo*-second-order model for the adsorption. Our Fe₃O₄NPs/CS/glyoxal/PVA hydrogel is hoped to serve as a promising Cr(VI) adsorbent in wastewater treatment technology.

Keywords: Chitosan; Adsorption; Pollutant; Chromium; Glyoxal; PVA

1. Introduction

The presence of high amounts of various heavy metals in waste matters is considered harmful to human health and environment [1]. Contamination of water by toxic heavy metals through leakage of industrial wastewater is a worldwide environmental problem. Heavy metals ions, such as Cu²⁺, Pb²⁺, Hg²⁺, Zn²⁺, As⁵⁺ and Cr⁶⁺, are generally non-biodegradable, highly toxic, dangerous, and carcinogenic. Among various heavy metals, the latter is one of the most toxic pollutants generated by mining, leather tanning, cement, dye, electroplating, steel, metal alloys, photographic material, and metal corrosion inhibition [2,3]. In fact, chromium exists in trivalent Cr(III) and

hexavalent Cr(VI) states. The hexavalent form has been considered more hazardous to public health due to its mutagenic and carcinogenic properties [4]. Therefore, removal of Cr(VI) from natural waters and wastewater streams has great environmental relevance. A wide range of physical and chemical processes is available for the removal of chromium from wastewater such as filtration [5], electrochemical precipitation [6], adsorption [7,8], electrodeposition [9], and membrane systems or ion exchange process [10–12]. Among these methods, adsorption is one of the most economically favorable and a technically easy method [13].

Recently, many researchers have studied feasibility of using low-cost biomass for the removal of various dyes, such as chitosan [14–16], cellulose [17,18], *Rhizopus oryzae* [19]. Polyvinyl alcohol (PVA) is a water-soluble material containing many reactive hydroxyl

*Corresponding author.

groups. It has been extensively applied in biomedical and pharmaceutical fields due to its low cost, non-toxicity, biocompatibility, good mechanical strength, and chemical stability. Recently, a new and economical way to prepare macroreticular PVA foam has been developed in our lab to immobilize micro-organism for wastewater treatment [20]. However, the resulting PVA foam illustrated low adsorption for organic and inorganic pollutants. Chitosan (CS), poly(1 → 4)-2-amino-2-deoxy-β-D-glucan is usually obtained from waste biomass during seafood processing, mainly shells of crabs, shrimp, prawns, and krill [21]. Chitosan is a natural polymer which is biodegradable, biocompatible, and non-toxic. Various biomaterials based on chitosan have already been explored as excellent adsorbents for the removal of most kinds of metals from aqueous solutions since CS have three functional groups, i.e. two hydroxyl groups (–OH) and one amino group (–NH₂), per glucosamine unit [21]. However, pure CS materials have some obvious disadvantages such as poor chemical resistance, low mechanical strength, and difficult recovery [14]. Besides great numbers of metals are preferentially adsorbed in acidic media while CS can be dissolved in acidic medium. To overcome such problems, some cross-linking agents such as glutaraldehyde [22], epichlorohydrin (ECH) [23], and ethyleneglycol diglycidyl ether [24] are used to improve mechanical and chemical properties of the resulting composite and prevent its dissolution in acidic solutions. In many studies, ECH is used as a cross-linking agent, for instance, insertion of ECH in magnetic chitosan nanoparticles has boosted the removal of Cr(VI) from aqueous solution with maximum adsorption capacity of 55.80 mg g⁻¹ in optimal adsorption conditions [25]. Yet, rather expensive ECH was a highly reactive flammable liquid which in contact with water hydrolyzed to highly carcinogenic 3-monochloropropane-1,2-diol or 3-chloropropane-1,2-diol [26]. Many reports take advantage of glyoxal as a cross-linking agent for various biomedical applications [27,28]. In addition, the adsorption capacity for cross-linked CS is lower when compared with free CS because of functional group (–NH₂) being cross-linked [29,30]. Blending of two or more polymers has increasingly become an important technique for improving the cost-performance ratio of commercial products [31]. PVA has been used in many biomaterial applications [32]. Since CS contains high contents of amino and hydroxyl functional groups, it may potentially be miscible with PVA because of the formation of hydrogen bonds [33,34]. Blended CS with PVA has been reported to have good mechanical and chemical properties. Specific intermolecular interactions between PVA and CS have

encouraged extensive studies in water treatment [34–36] and drug-controlled releases [37].

On the other hand, after the adsorption is carried out, the adsorbents are difficult to be separated from the solution using traditional separation methods such as filtration and sedimentation. Magnetic carriers are used as the support material and they can be easily separated from the reaction medium and stabilized in a fluidized bed reactor by applying a magnetic field [25].

In this paper, novel Fe₃O₄NPs/CS/glyoxal/PVA hydrogel film was prepared, characterized, and applied for the removal of Cr(VI) from water, in the range of 5–30 ppm as initial chromium concentrations. Afterwards, the effects of the process parameters such as pH, temperature, initial Cr(VI) concentration on Cr(VI) removal were investigated. In order to understand the adsorption characteristic, the isotherm, kinetic, and thermodynamic models were employed for the evaluation of the adsorption process.

2. Materials and methods

2.1. Materials

Analytical grade FeCl₃·6H₂O, FeCl₂·4H₂O, K₂Cr₂O₇, CH₃COOH, HCl, and NaOH were obtained from Merck. Chitosan (CS, degree of deacetylation = 82 ± 2%, Mw = 100,000–300,000 g mol⁻¹) was purchased from Acros Organics Company and used without any post-modification. Polyvinyl alcohol (PVA, Mw = 72,000 g mol⁻¹, degree of hydrolysis was 98.0%) was purchased from Merck Company. Glyoxal (~40% content in water, ~8.8 M) was also purchased from Merck Company. Double distilled water was used for preparation of all solutions.

2.2. Preparation of magnetic chitosan/glyoxal/PVA hydrogel film

2.2.1. Fabrication of Fe₃O₄ nanoparticles

Fe₃O₄ nanoparticles have been prepared using the reported standard protocol of coprecipitating FeCl₂ with FeCl₃ in water and sodium hydroxide [38]. Specifically, FeCl₂·4H₂O and FeCl₃·6H₂O were taken in molar ratio of 1:2 in 100-mL water. Then, 4-M NaOH was added slowly until pH reached 12 at 95°C. After continuous stirring and aging for 2 h, the mixture was filtered, washed, and dried at 60°C for 12 h.

2.2.2. Using Fe₃O₄ nanoparticles in preparation of the adsorbent

Fifty-milligram chitosan was dissolved in 5-mL acid acetic 2% (V/V). To it 50-mg Fe₃O₄ nanoparticles

was added and dispersed by sonicating for 2 h. After that 22- μ L glyoxal was added then sonicated again for 1 h. In another flask, 100-mg PVA was dissolved in 10-mL distilled water at 70°C. The two solutions were mixed and stirred magnetically. Then, 300 ml NaOH 0.1 M was added. The resulting hydrogel turned into a brown film, upon overnight drying in the oven at 60°C. In order to remove the unreacted chitosan and glyoxal, the film was rinsed with acetic acid (3 times) and distilled water (2 times), at 0 and 100°C; then finally it was dried in the oven at 60°C.

2.3. Adsorption experiments

The sorption experiments were performed via a batch method. Samples of 0.05 g of Fe₃O₄NPs/CS/glyoxal/PVA hydrogel were equilibrated with 50 mL of solution containing various amounts of Cr(VI). The pH was adjusted using 1-M solutions of NaOH and HCl. The experiments were performed at different temperatures (25, 35, and 45°C). Adsorption isotherms of Cr(VI) over Fe₃O₄NPs/CS/glyoxal/PVA hydrogel were measured at these temperatures. Such sorption isotherms were plots of the equilibrium adsorption capacity (q_e) (according to Eq. (1)) vs. the equilibrium concentration of the residual Cr(VI) in the solution (C_e) [39].

$$q_e = \frac{(C_0 - C_e)V}{W} \quad (1)$$

Here q_e is the equilibrium adsorption capacity (mg g^{-1}), C_0 and C_e are the initial and equilibrium liquid phase solute concentration (mg L^{-1}), respectively. V is the liquid phase volume (L) and W is amount of the adsorbent (g). Residual concentrations of Cr(VI) are determined with an inductively coupled plasma optical emission spectrometer (ICP-OES).

2.4. Characterization methods

FT-IR spectra were recorded using Perkin-Elmer 597 and Nicolet 510P spectrophotometers. Crystal structures were examined using a Holland Philips Xpert X-ray powder diffraction (XRD) diffractometer (Cu K α , radiation, $\lambda = 0.154056$ nm), at a scanning speed of 2°/min from 10° to 80° (2θ). Morphologies were obtained using scanning electron microscopy (SEM) of a Holland Philips XL30 microscope with an accelerating voltage of 22 kV. Elemental microanalysis was carried out using a Philips XL30 energy dispersive X-ray analysis (EDX), operating at 17.0 kV.

3. Results and discussion

We characterized our novel adsorbent (Fe₃O₄NPs/CS/glyoxal/PVA hydrogel) through FT-IR, XRD, SEM, and EDX analyses. Then, the effect of initial pH on the Cr(VI) adsorption process was probed. Subsequently, studies on adsorption isotherm, thermodynamic and kinetic studies, along with reusability of the adsorbent were discussed.

Pure CS materials have some obvious disadvantages such as poor chemical resistance, low mechanical strength, and difficult recovery [14]. In this work, we have used both glyoxal and PVA to improve the mechanical and chemical properties of our adsorbent (Fe₃O₄NPs/CS/glyoxal/PVA). As a constituent of the latter, PVA makes it more water soluble for containing many reactive hydroxyl groups. Besides, PVA is economical, non-toxic, and biocompatible, with good mechanical strength and chemical stability. On the other hand, glyoxal was used to improve mechanical and chemical properties of our composite and prevent CS from dissolution in acidic solutions. In addition, the adsorption capacity for cross-linked CS is lower when compared with free CS, because of functional group ($-\text{NH}_2$) being cross-linked [29,30]. Hence, blending of CS, glyoxal, and PVA was aimed to improve the adsorption capacity and cost-performance ratio of our adsorbent [31].

Coexistence of CS and PVA in the presence of glyoxal might have brought confusion as to whether the adsorbent in this work was the hydrogel film or the mixed hydrogel. The possibility of the latter might be ruled out by considering the order of addition of the starting materials. Glyoxal was added to the magnetic chitosan solution and sonicated for 1 h before PVA was added. Considering such order of addition, the very low amount of the employed glyoxal, and the higher viscosity encountered upon such addition, one could conclude that all glyoxal was spent in cross linking of the amino groups of CS (Fig. 1) [28]. Also, addition of PVA to the resulting magnetic chitosan/glyoxal has not rendered any covalent linkages but has provided hydrogen bridges between chitosan and PVA.

3.1. Characterization of the adsorbent

3.1.1. FT-IR analysis

Characteristic Fe–O absorption bands in FT-IR spectra of Fe₃O₄NPs, and Fe₃O₄NPs/CS/glyoxal/PVA appeared at 567.36 and 570.77 cm^{-1} , respectively (Fig. 2(a) and (b)). Other adsorption peaks of the latter included those at 1,000–1,200 cm^{-1} (C–N stretchings)

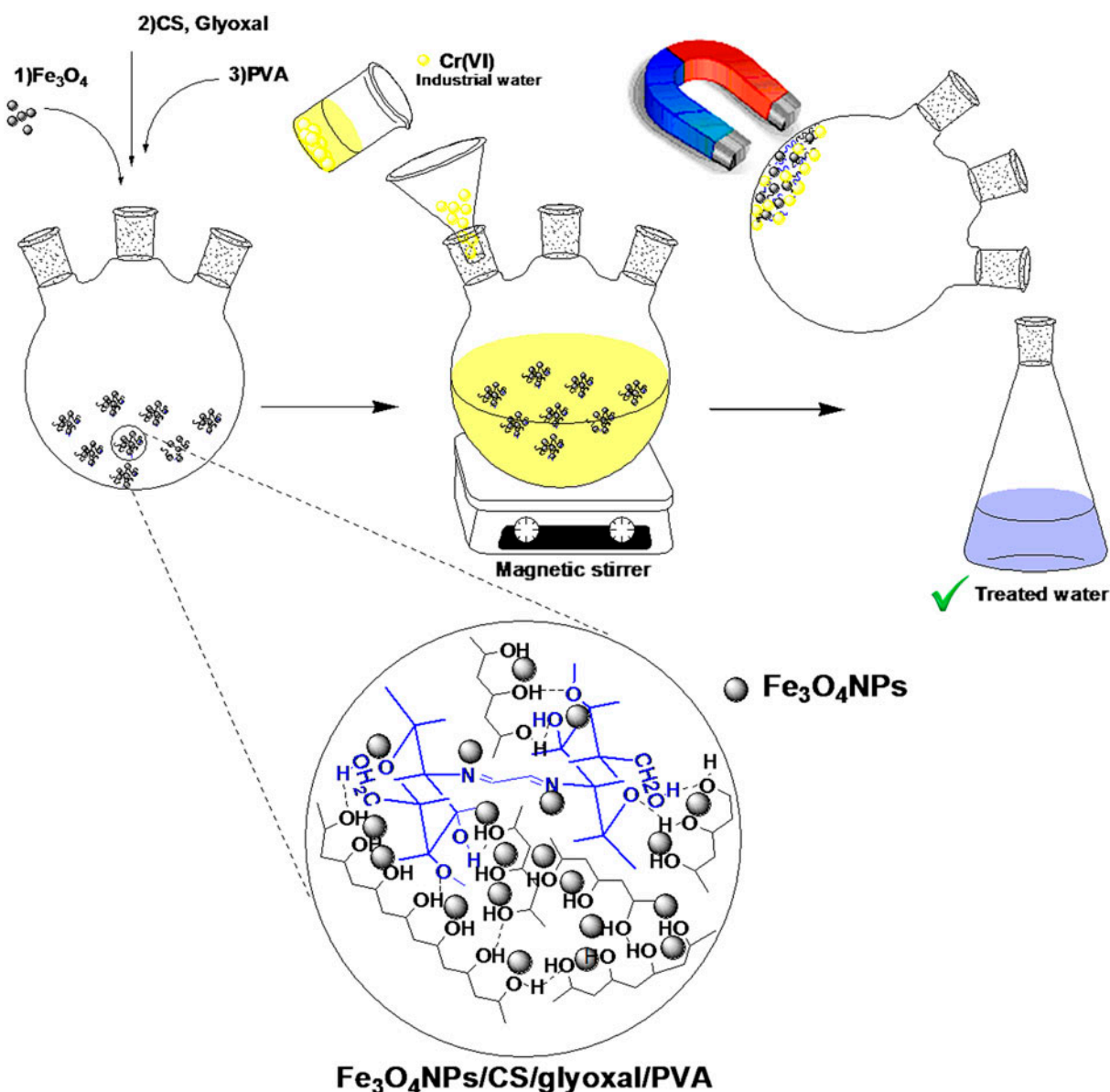


Fig. 1. Removal of Cr(VI) over $\text{Fe}_3\text{O}_4\text{NPs}/\text{CS}/\text{glyoxal}/\text{PVA}$ absorbent film. Glyoxal has cross linked amine groups of CS, while PVA has acted as a chelating agent.

[40], $1,263.37\text{ cm}^{-1}$ (C–O stretching), $1,520.25$ and $1,641.28\text{ cm}^{-1}$ (N–H bending vibrations) [41], $2,925.09$ and $2,855.84\text{ cm}^{-1}$ (C–H stretchings), $3,443.06\text{ cm}^{-1}$ (O–H and N–H stretchings). However, the anticipated glyoxal carbonyl adsorption peak at $1,720\text{--}1,740\text{ cm}^{-1}$ [42] was not seen. This was due to its Schiff base reaction with the amine group of chitosan [43,44], forming an imine with absorption vibration at $1,660\text{ cm}^{-1}$, due to C=N stretching [28]. The latter appeared as a shoulder on a broad peak caused by the N–H bending vibration. The peak at $2,359\text{ cm}^{-1}$ in the FT-IR of the absorbent may correspond to the mono-linked

glyoxal-chitosan where the possibility of a triple bond of carbon is anticipated (Scheme 1). Reaction of glyoxal with chitosan amino group of the first chain is fast while its reaction with the second chain is time requiring and slow. Hence, a decrease in the intensity at $2,359\text{ cm}^{-1}$ is observed through time (Fig. 2(b) and (c)).

3.1.2. XRD analysis

XRD analysis was carried out on Fe_3O_4 NPs and Fe_3O_4 NPs/CS/glyoxal/PVA hydrogel film (before

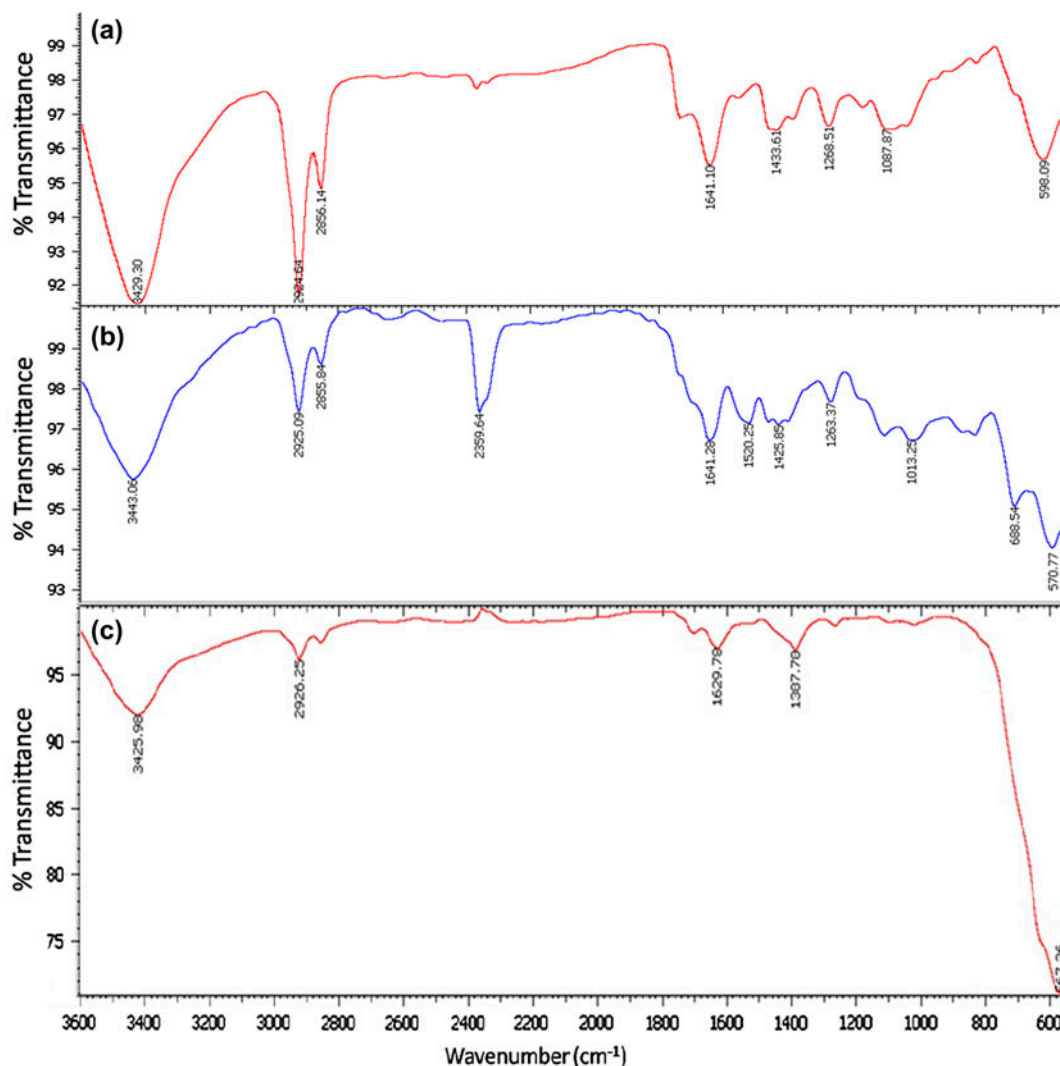


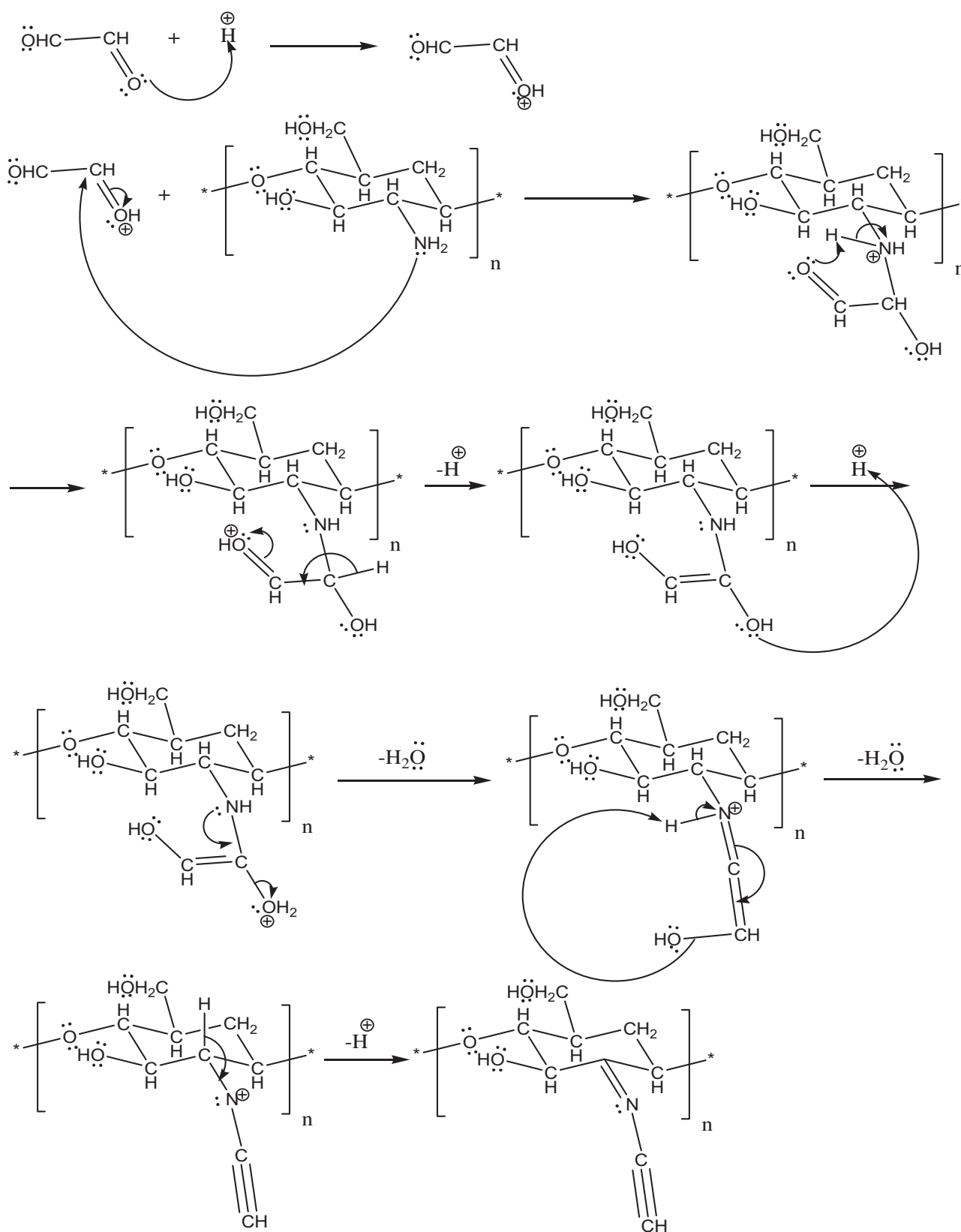
Fig. 2. FT-IR spectra of $\text{Fe}_3\text{O}_4\text{NPs}$ (a); $\text{Fe}_3\text{O}_4\text{NPs}/\text{CS}/\text{glyoxal}/\text{PVA}$ hydrogel (b and c).

and after chromium adsorption) (Fig. 3). The main peaks of $\text{Fe}_3\text{O}_4\text{NPs}$ appeared at $2\theta = 35.45^\circ$, 41.83° , 51.01° , 63.65° , 68.02° , and 75.02° , corresponding to the (2 2 0), (3 1 1), (4 0 0), (4 2 2), (5 1 1), and (4 4 0) crystal planes of pure Fe_3O_4 with a cubic structure, respectively [45–47]. At the same time, it could be seen that the strong characteristic diffraction peaks of Fe_3O_4 ((2 2 0), (3 1 1), (4 0 0), (5 1 1), and (4 4 0)) could be found in the pattern of $\text{Fe}_3\text{O}_4\text{NPs}/\text{CS}/\text{glyoxal}/\text{PVA}$ hydrogel, before adsorption. The diffraction peaks between $2\theta = 20^\circ$ and $2\theta = 30^\circ$ were associated with chitosan and PVA. They had amorphous nature indicating a low crystallinity [36,48,49]. The above results indicated that the film had been prepared successfully without damaging the crystal structure of $\text{Fe}_3\text{O}_4\text{NPs}$. With the same token, after chromium adsorption, $\text{Fe}_3\text{O}_4\text{NPs}$ was not damaged (Fig. 3(c)). Hence, particle

sizes of the film before and after adsorption of 5 ppm initial chromium concentration under the optimum condition were estimated approximately as 12.85 and 20.99 nm, respectively. These were extracted from considering line broadenings in the pattern, and using Debye–Scherrer equation ($d = k\lambda/\beta \cos \theta$), at $2\theta = 41.63^\circ$.

3.1.3. SEM analysis

Before subjecting our absorbent to Cr(VI) contaminated water, rather sharp spherical $\text{Fe}_3\text{O}_4\text{NPs}/\text{CS}/\text{glyoxal}/\text{PVA}$ hydrogel was observed in its SEM image (Fig. 4(a)). After subjecting our absorbent to Cr(VI) contaminated water, the latter seemed to form a thin fussy layer over the absorbent, making it appear with an increase in the size of $\text{Fe}_3\text{O}_4\text{NPs}$ (Fig. 4(b)).



Scheme 1. Mono linked glyoxal-chitosan that the possibility of a triple bond of carbon is anticipated.

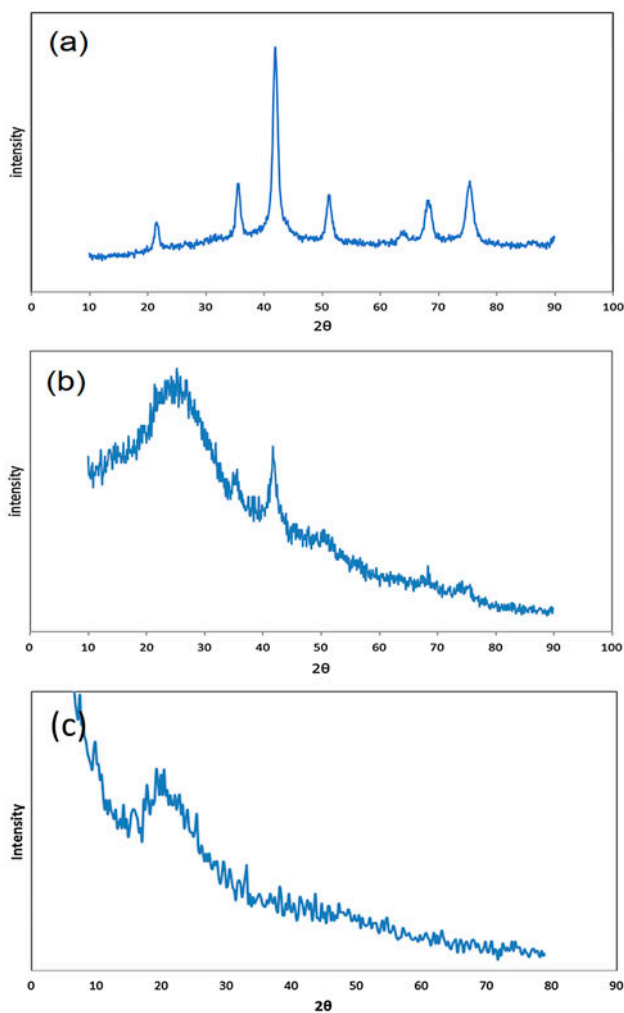


Fig. 3. XRD patterns of Fe₃O₄NPs (a), along with those of Fe₃O₄NPs/CS/glyoxal/PVA hydrogel film, before (b), and after chromium adsorption (c).

3.1.4. EDX analysis

The EDX analysis of the film before absorption showed no trace of Cr (Fig. 5(a)). Its spectrum after contact with 5 ppm initial chromium concentration (in optimum condition) showed 2.03 W% of Cr (Fig. 5(b)).

3.2. Effect of initial pH on the adsorption process

Perhaps, the most important parameter which controlled the metal ion adsorption process was pH. It significantly influenced the surface charge and the protonation degree of the adsorbent in the solution. Depending on the solution pH and total chromate concentration, Cr(VI) appeared with different ionic forms: CrO₄²⁻, Cr₂O₇²⁻, HCrO₄⁻, etc. [50]. Adsorption

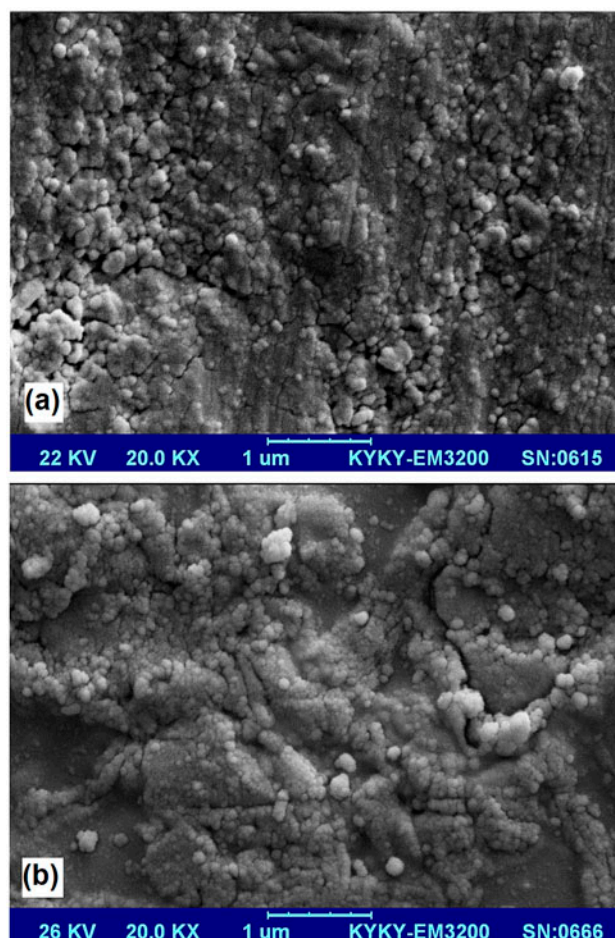


Fig. 4. SEM images of our adsorbent, Fe₃O₄NPs/CS/glyoxal/PVA hydrogel before adsorption (a) and after chromium adsorption (b).

process was investigated at pH 2.0–8.0. The maximum capacity of Cr(VI) absorption occurred at pH 3.0 (Fig. 6). The pH of the aqueous solution may have affected both the stability of chromium species involved and the surface charge of the adsorbent [51]. The adsorption of Cr(VI) increased proportionally with an increase of pH from 2.0 to 3.0. Specifically, [H₂Cr₂O₇] decreased as [HCrO₄⁻] increased. The amino groups (–NH₂) of Fe₃O₄NPs/CS/glyoxal/PVA hydrogel, which had not reacted with glyoxal, appeared in the acidic solution with a protonated cationic form (–NH₃⁺) [52–54]. Electrostatic interaction between the sorbent and HCrO₄⁻ ions also contributed to the high chromium removal. However, at pH lower than 3.0, a decrease in the uptake capacity was observed due to the strong competition for adsorption sites between H₂CrO₄ and protons. Besides, as the pH increased, there was competition

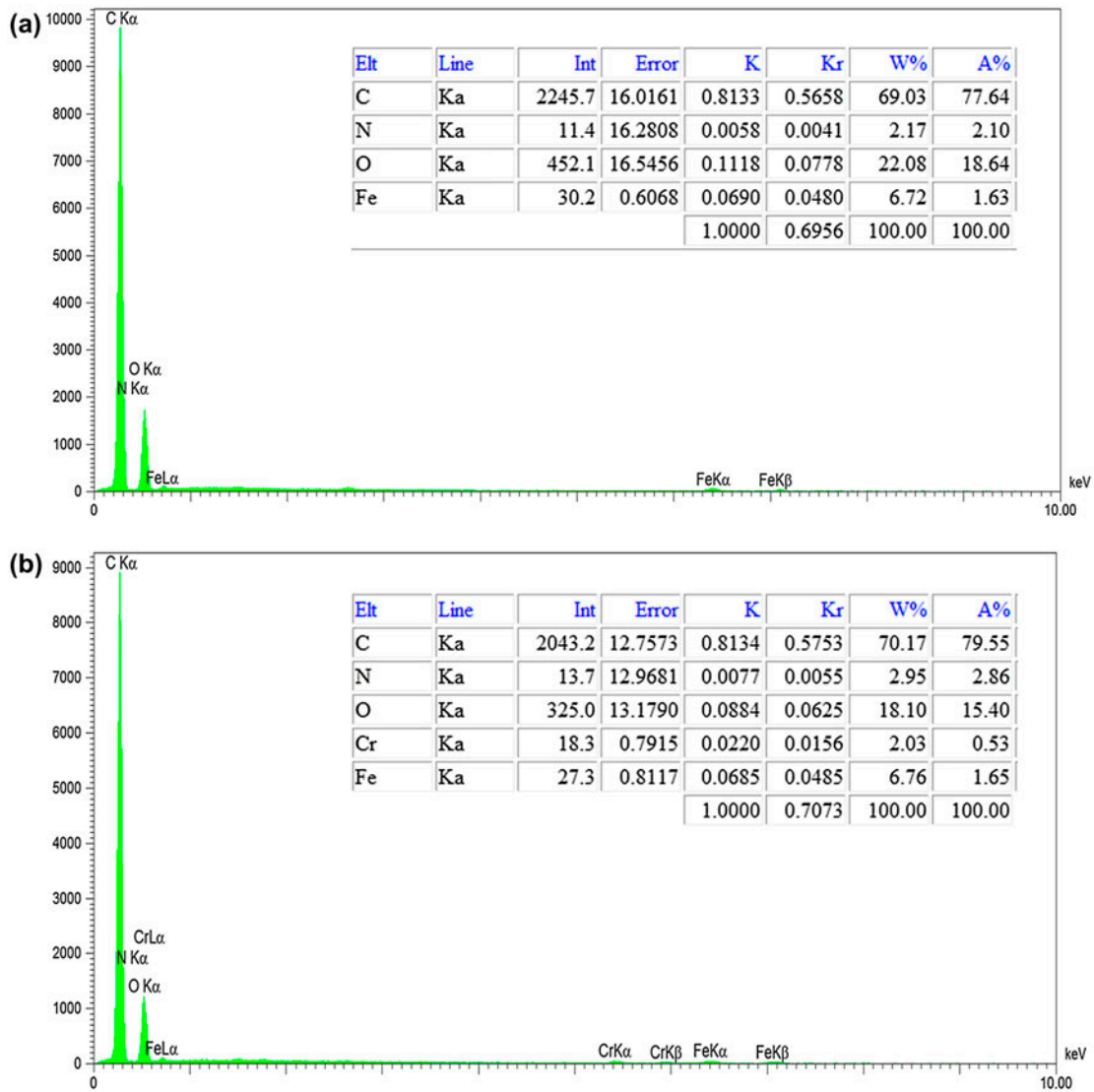


Fig. 5. EDX patterns of our adsorbent, Fe₃O₄NPs/CS/glyoxal/PVA hydrogel before adsorption (a) and after chromium adsorption (b).

between OH⁻ and chromate ions, especially at high pH levels [25,55].

3.3. Adsorption isotherms

Equilibrium experimental data were successfully fitted to the Langmuir isotherm whose equation could be expressed as [56]:

$$\frac{C_e}{q_e} = \frac{1}{bq_m} + \frac{C_e}{q_m} \quad (2)$$

where q_e (mg g⁻¹) is the amount of solution adsorbed per unit mass of the adsorbent, C_e (mg L⁻¹) is the solute equilibrium concentration, q_m (mg g⁻¹) is the maximum adsorbate amount that formed a complete monolayer on the surface, and b (L mg⁻¹) is the Langmuir constant related to adsorption heat. When C_e/q_e was plotted against C_e and the data were regressed linearly, the q_m and b constants could be calculated from the slope and the intercept. The efficiency of the adsorption could be expressed by the dimensionless equilibrium parameter R_L , which was defined as follows [56]:

$$R_L = \frac{1}{1 + bC_0} \quad (3)$$

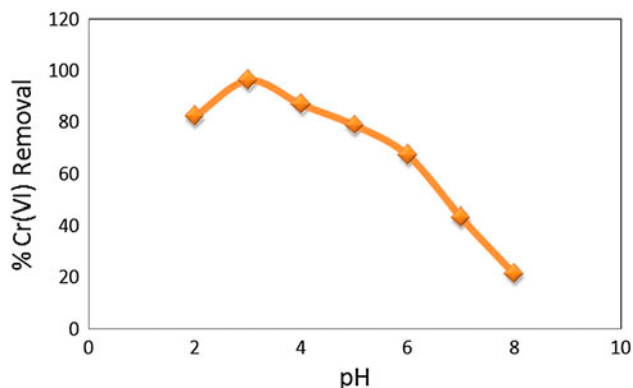


Fig. 6. Effect of pH on removal of Cr(VI) (metal concentration = 15 mg L⁻¹, adsorbent dose = 0.05 g, contact time = 90 min, temperature = 25 °C).

Table 1

Adsorption equilibrium constants obtained from Langmuir isotherm in the adsorption of Cr(VI) onto Fe₃O₄NPs/CS/glyoxal/PVA hydrogel (volume = 50 mL; adsorbent dose = 0.05 g; initial concentrations = 5, 10, 15, 20, 25, and 30 mg L⁻¹; pH 3.0; contact time 90 min; temperature = 298, 308, 318 K)

| Temperature (K) | q_m (mg g ⁻¹) | b | R^2 | R_L |
|-----------------|-----------------------------|-------|-------|-------|
| 298 | 33.78 | 1.281 | 0.995 | 0.025 |
| 308 | 28.57 | 0.778 | 0.993 | 0.041 |
| 318 | 22.27 | 0.681 | 0.997 | 0.047 |

where b (L mg⁻¹) is the Langmuir constant and C_0 is the initial Cr(VI) concentration (mg L⁻¹). Values of R_L indicated the isotherm shapes, which could be unfavorable ($R_L \gg 1$) or favorable ($0 << R_L << 1$) [57].

Table 2

Comparison between maximum adsorption capacities of Cr(VI) on Fe₃O₄NPs/CS/glyoxal/PVA and other adsorbents

| Adsorbents | Adsorption capacity (mg g ⁻¹) | Initial chromium concentration (ppm) | pH | Ref. |
|---|---|--------------------------------------|-----|--------------|
| Magnetic nanoparticles | 3.55 | 5–15 | 2.0 | [58] |
| Alginate/polyvinyl alcohol-hematite composite | 12.50 | 10–200 | 4.5 | [59] |
| Chitosan | 22.09 | 15–95 | 3.0 | [25] |
| Cross linked chitosan | 50.00 | 10–1,000 | 5.0 | [25] |
| Non-cross linked chitosan | 78.00 | 10–1,000 | 5.0 | [25] |
| Magnetic chitosan nanoparticles | 55.80 | 40–180 | 3.0 | [25] |
| Biofunctional magnetic bead | 6.97 | 5–200 | 1.0 | [59] |
| Ethylenediamine-modified cross-linked magnetic chitosan resin | 51.81 | 20–200 | 2.0 | [39] |
| Biopolymeric beads of sodium alginate | 16.67 | 5–25 | 4.0 | [59] |
| Fe ₃ O ₄ NPs/CS/glyoxal/PVA | 33.78 | 5–30 | 3 | Present work |

The experimental data fitted well with Langmuir model ($R^2 > 0.99$), confirming that the adsorption process was monolayer and the values of R_L were favorable (Table 1). The q_m value for Cr(VI) on Fe₃O₄NPs/CS/glyoxal/PVA hydrogel was compared with those reported previously using different adsorbents (Table 2). One might have wondered what was the main advantage for Fe₃O₄NPs/CS/glyoxal/PVA hydrogel compared with other similar adsorbents with relative high adsorption capacities, since the maximum adsorption capacities of Cr(VI) on Fe₃O₄NPs/CS/glyoxal/PVA have appeared much less than magnetic chitosan nanoparticles and other similar adsorbents. Yet, the absorption capacity is highly dependent on initial concentration [58], and our Fe₃O₄NPs/CS/glyoxal/PVA has a higher absorption capacity than reported adsorbents within the employed initial concentration range of 5–30 ppm, at pH 3.

The equilibrium isotherms for the adsorption of Cr(VI) onto Fe₃O₄NPs/CS/glyoxal/PVA hydrogel at different temperatures (25, 35, and 45 °C) at pH 3.0 were considered (Fig. 7).

3.4. Effect of adsorption time and adsorbent dose

Removal of Cr(VI) was probed with an initial adsorbent concentration of 15 mg L⁻¹ against the adsorption time (Fig. 8(a)). The results showed an increase of Cr(VI) adsorption with increasing contact time. Specifically, in order to ensure that adsorption process could reach the equilibrium, the contact time was set at 90 min. The removal percent was 96.29% for the 15 mg L⁻¹ initial Cr(VI) solution.

The effect of adsorbent dose on the removal efficiency (% removal) of Cr(VI) was studied (Fig. 8(b)).

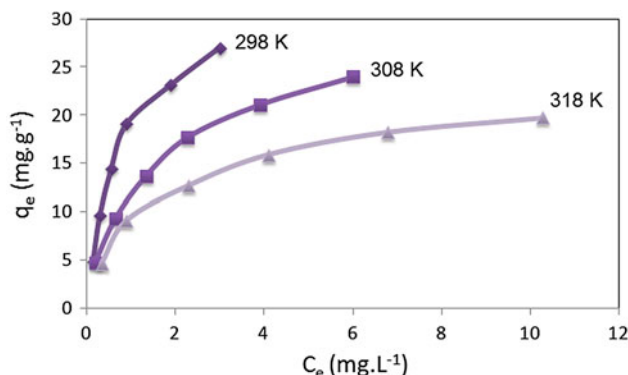


Fig. 7. Adsorption isotherms of Cr(VI) onto Fe₃O₄NPs/CS/glyoxal/PVA at 25, 35, and 45°C (adsorbent dose = 0.05 g; volume of the medium = 50 mL; pH 3.0 and contact time = 90 min).

The removal efficiency raised from 59.79 to 96.29% as the dosage of Fe₃O₄NPs/CS/glyoxal/PVA was increased from 20.0 to 50.0 mg. This trend suggested more active sites becoming available with an increase in the adsorbent dose.

3.5. Thermodynamic and kinetic studies

Thermodynamic parameters of the adsorption process, such as the change in standard free energy (ΔG), enthalpy (ΔH), and entropy (ΔS) could be obtained using the following equations [25,39]:

$$\Delta G = \Delta H - T \cdot \Delta S \quad (4)$$

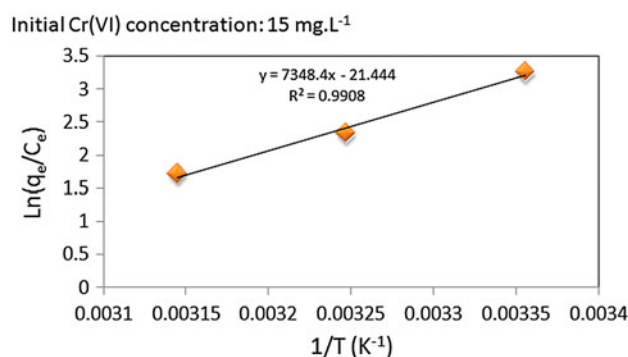


Fig. 9. Thermodynamic plot of $\ln(q_e/C_e)$ vs. $1/T$.

$$\ln b = \ln\left(\frac{q_e}{C_e}\right) = -\frac{\Delta H}{RT} + \frac{\Delta S}{R} \quad (5)$$

where b is the Langmuir constant ($L \text{ mol}^{-1}$), R is the ideal gas constant ($8.31 \text{ J mol}^{-1} \text{ K}^{-1}$), and T is the absolute temperature (K). ΔH and ΔS were obtained from the slope and intercept of the plot $\ln(q_e/C_e)$ vs. $1/T$ (Fig. 9), namely:

$$\Delta H = -61.094 \text{ (kJ mol}^{-1}\text{)} \text{ and } \Delta S = -0.178 \text{ (kJ mol}^{-1} \text{ K}^{-1}\text{)}.$$

The negative values of the ΔG and ΔH mean the adsorption were an exothermic spontaneous process (Table 3). Consequently, a lower temperature increased the adsorption and q_m . The negative ΔH was noteworthy, since Li et al. [60] and Bayramoglu [61] have reported a positive ΔH for Cr(VI)

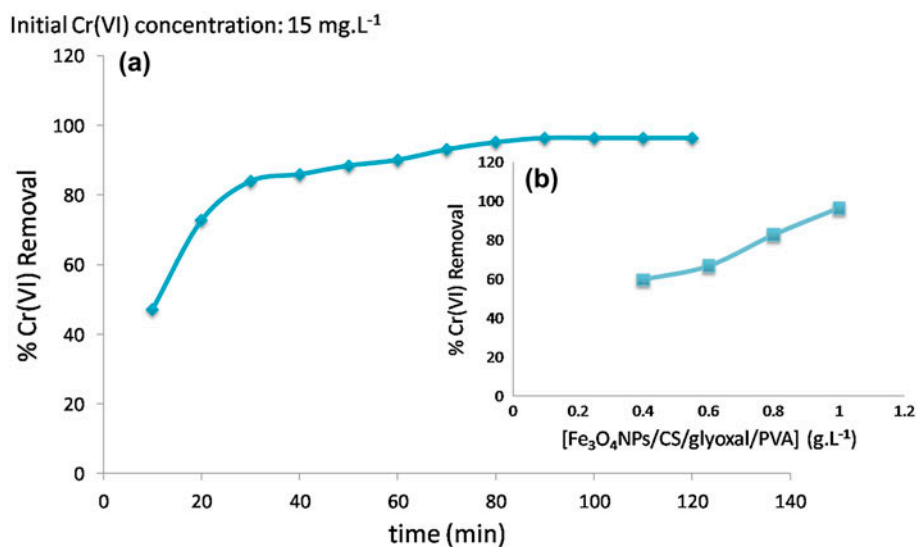


Fig. 8. % Removal of Cr(VI) at pH 3 and temperature = 25°C as functions of: (a) the contact time, at adsorbent dose = 0.05 g and (b) concentration of the adsorbent (Fe₃O₄NPs/CS/glyoxal/PVA hydrogel), at contact time = 90 min.

Table 3
Thermodynamic data of Cr(VI) adsorption process

| T (K) | ΔG (kJ mol ⁻¹) | ΔH (kJ mol ⁻¹) | ΔS (kJ mol ⁻¹ K ⁻¹) |
|-------|------------------------------------|------------------------------------|--|
| 298 | -8.050 | -61.094 | -0.178 |
| 304 | -6.982 | | |
| 310 | -5.914 | | |
| 316 | -4.846 | | |

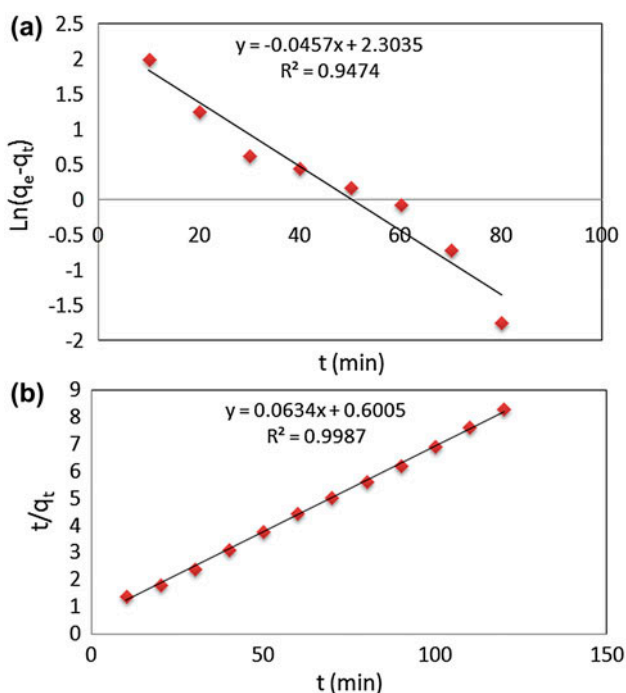


Fig. 10. Kinetic studies with volume = 50 mL, adsorbent dose = 0.05 g, initial concentrations = 15 mg L⁻¹, pH 3.0, at temperature = 298 K; for *Pseudo*-first-order adsorption (a), and *pseudo*-second-order adsorption (b), where q_e and q_t were the amounts of Cr(VI) (mg g⁻¹) adsorbed on the adsorbent at equilibrium and at time t .

adsorption. A negative value for ΔS indicated that the degree order increased during the adsorption process.

Pseudo-first-order and the *pseudo*-second-order kinetics were applied to the experimental data

(Fig. 10). The *pseudo*-first-order rate expression of Lagergren was given as [62]:

$$\ln(q_e - q_t) = \ln(q_e) - k_1 \cdot t \quad (6)$$

where q_e and q_t were the amounts of Cr(VI) (mg g⁻¹) adsorbed on the adsorbent at equilibrium and at time t , respectively and k_1 was the rate constant of first-order adsorption (min⁻¹). The slopes and intercepts of plots of $\ln(q_e - q_t)$ vs. t were used to determine the first-order rate constant k_1 . The *pseudo*-second-order kinetic model was expressed through the following equation [62]:

$$\frac{t}{q_t} = \frac{1}{k_2 \cdot q_e^2} + \frac{1}{q_e} \cdot t \quad (7)$$

where k_2 (g mg⁻¹ min⁻¹) is the rate constant of second-order adsorption. The slopes and intercepts of plots of t/q_t vs. t were used to calculate the second-order rate constant k_2 and q_e . The value of regression coefficient (R^2) for *pseudo*-second-order Cr model was close to 1 (0.999) for 15 mg L⁻¹ initial Cr(VI) concentration (Table 4). The calculated value $q_{e,cal}$ was very close to the obtained $q_{e,exp}$ value. Hence, the adsorption of Cr(VI) onto Fe₃O₄NPs/CS/glyoxal/PVA hydrogel could obey the *pseudo*-second-order kinetic model.

3.6. Reusability of Fe₃O₄NPs/CS/glyoxal/PVA hydrogel

Our novel Fe₃O₄NPs/CS/glyoxal/PVA hydrogel has demonstrated its adsorption ability during three adsorption cycles (Fig. 11). After three cycles, the Cr (VI) adsorption capacity decreased from initial 84.24% to the final 53.91%. This behavior indicated that the Fe₃O₄NPs/CS/glyoxal/PVA hydrogel could be applied, at least three times, for rather efficient Cr(VI) adsorption, from aqueous solutions. Specifically, 0.1-M HCl solution was used as desorption agent. Although the reusability of Fe₃O₄NPs/CS/glyoxal/PVA

Table 4

Kinetic studies, where k_1 and k_2 were the first- and second-order rate constants; $q_{e,cal}$ and $q_{e,exp}$ were the calculated and experimental quantities of Cr(VI) (mg g⁻¹) adsorbed; R^2 was the regression coefficient

| $q_{e,exp}$ (mg g ⁻¹) | Pseudo-first-order mode | | | Pseudo-second-order mode | | |
|-----------------------------------|----------------------------|-----------------------------------|-------|---|-----------------------------------|-------|
| | k_1 (min ⁻¹) | $q_{e,cal}$ (mg g ⁻¹) | R^2 | k_2 (g mg ⁻¹ min ⁻¹) | $q_{e,cal}$ (mg g ⁻¹) | R^2 |
| 14.44 | 4.57×10^{-2} | 10.01 | 0.947 | 6.69×10^{-3} | 15.77 | 0.999 |

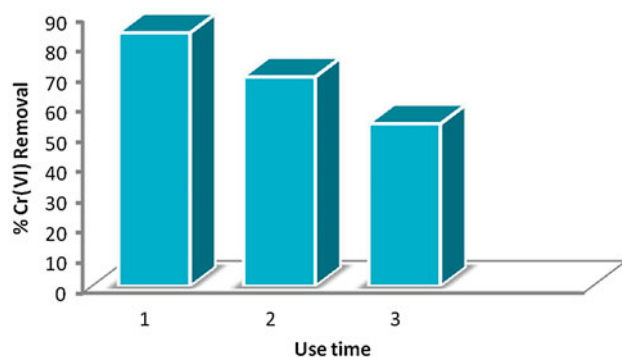


Fig. 11. Adsorption performance of $\text{Fe}_3\text{O}_4\text{NPs}/\text{CS}/\text{glyoxal}/\text{PVA}$ hydrogel in three cycles.

hydrogel has appeared still not so ideal, one may reduce Cr(VI) initial concentration from 5–30 ppm to 0.08–0.48 ppm after three runs. This solution did not harm our CS for it was strongly cross-linked with glyoxal.

4. Conclusion

The present study focused on adsorption of Cr(VI) from aqueous solutions using the $\text{Fe}_3\text{O}_4\text{NPs}/\text{CS}/\text{glyoxal}/\text{PVA}$ hydrogel as an efficient and novel adsorbent. Ambient adsorption of Cr(VI) was found to be more effective at a lower pH range. Optimum adsorption conditions of Cr(VI) were found at pH 3, contact time of 90 min, and with maximum adsorption capacity of 33.78 mg g^{-1} . The Langmuir model was found to fit well with the experimental data (correlation coefficient $R^2 > 0.99$), indicating the occurrence of monolayer adsorption process. Thermodynamically, the adsorption of Cr(VI) was spontaneous (in term of ΔG) and exothermic (in term of ΔH) process. The kinetic data of the adsorption under 15-mg L^{-1} initial concentration fitted well with the *pseudo*-second-order kinetic model. In addition, the fast adsorption and settling for the $\text{Fe}_3\text{O}_4\text{NPs}/\text{CS}/\text{glyoxal}/\text{PVA}$ hydrogel made this material a possible candidate for continuous flow water treatment systems. The mechanism of adsorption included mainly ionic interactions (chemical interactions) and electrostatic interactions (physical interactions) between metal cations and $\text{Fe}_3\text{O}_4\text{NPs}/\text{CS}/\text{glyoxal}/\text{PVA}$ hydrogel, so this adsorption was a physicochemical process.

Supplementary material

The supplementary material for this paper is available online at <http://dx.doi.org/10.1080/19443994.2015.1065763>.

References

- [1] X. Ren, C. Chen, M. Nagatsu, X. Wang, Carbon nanotubes as adsorbents in environmental pollution management: A review, *Chem. Eng. J.* 170 (2011) 395–410.
- [2] P.G. Gopi Krishna, J.M. Gladis, U. Rambabu, T.P. Rao, G.R.K. Naidu, Preconcentrative separation of chromium(VI) species from chromium(III) by coprecipitation of its ethyl xanthate complex onto naphthalene, *Talanta* 63 (2004) 541–546.
- [3] R.L. Ramos, A.J. Martinez, R.M.G. Coronado, Adsorption of chromium(VI) from aqueous solutions on activated carbon, *Water Sci. Technol.* 30 (1994) 191–197.
- [4] S. Basha, Z.V.P. Murthy, B. Jha, Biosorption of hexavalent chromium by chemically modified seaweed, *Cystoseira indica*, *Chem. Eng. J.* 137 (2008) 480–488.
- [5] C. Das, P. Patel, S. De, S. DasGupta, Treatment of tanning effluent using nanofiltration followed by reverse osmosis, *Sep. Purif. Technol.* 50 (2006) 291–299.
- [6] N. Kongsricharoern, C. Polprasert, Chromium removal by a bipolar electro-chemical precipitation process, *Water Sci. Technol.* 34 (1996) 109–116.
- [7] E.S. Abdel-Halim, S.S. Al-Deyab, Hydrogel from cross-linked polyacrylamide/guar gum graft copolymer for sorption of hexavalent chromium ion, *Carbohydr. Polym.* 86 (2011) 1306–1312.
- [8] Q. Li, Y. Qian, H. Cui, Q. Zhang, R. Tang, J. Zhai, Preparation of poly(aniline-1,8-diaminonaphthalene) and its application as adsorbent for selective removal of Cr(VI) ions, *Chem. Eng. J.* 173 (2011) 715–721.
- [9] J. Liu, C. Wang, J. Shi, H. Liu, Y. Tong, Aqueous Cr(VI) reduction by electrodeposited zero-valent iron at neutral pH: Acceleration by organic matters, *J. Hazard. Mater.* 163 (2009) 370–375.
- [10] R. Güell, E. Anticó, V. Salvadó, C. Fontàs, Efficient hollow fiber supported liquid membrane system for the removal and preconcentration of Cr(VI) at trace levels, *Sep. Purif. Technol.* 62 (2008) 389–393.
- [11] F. Gode, E. Pehlivan, Removal of Cr(VI) from aqueous solution by two Lewatit-anion exchange resins, *J. Hazard. Mater.* 119 (2005) 175–182.
- [12] T. Sardohan, E. Kir, A. Gulec, Y. Cengeloglu, Removal of Cr(III) and Cr(VI) through the plasma modified and unmodified ion-exchange membranes, *Sep. Purif. Technol.* 74 (2010) 14–20.
- [13] T. Karthikeyan, S. Rajgopal, L.R. Miranda, Chromium (VI) adsorption from aqueous solution by sawdust activated carbon, *J. Hazard. Mater.* 124 (2005) 192–199.
- [14] L. Wang, A. Wang, Adsorption properties of congo red from aqueous solution onto N,O-carboxymethyl-chitosan, *Bioresour. Technol.* 99 (2008) 1403–1408.
- [15] G.L. Dotto, L.A.A. Pinto, Adsorption of food dyes onto chitosan: Optimization process and kinetic, *Carbohydr. Polym.* 84 (2011) 231–238.
- [16] H. Zhu, R. Jiang, L. Xiao, W. Li, A novel magnetically separable $\gamma\text{-Fe}_2\text{O}_3$ /crosslinked chitosan adsorbent: Preparation, characterization and adsorption application for removal of hazardous azo dye, *J. Hazard. Mater.* 179 (2010) 251–257.
- [17] G. Annadurai, R.S. Juang, D.J. Lee, Use of cellulose-based wastes for adsorption of dyes from aqueous solutions, *J. Hazard. Mater.* 92 (2002) 263–274.

- [18] X. Luo, L. Zhang, High effective adsorption of organic dyes on magnetic cellulose beads entrapping activated carbon, *J. Hazard. Mater.* 171 (2009) 340–347.
- [19] S.K. Das, J. Bhowal, A.R. Das, A.K. Guha, Adsorption Behavior of Rhodamine B on *Rhizopus oryzae* biomass, *Langmuir* 22 (2006) 7265–7272.
- [20] X. Bai, Z. Ye, Y. Li, L. Zhou, L. Yang, Preparation of crosslinked macroporous PVA foam carrier for immobilization of microorganisms, *Process Biochem.* 45 (2010) 60–66.
- [21] G. Crini, Non-conventional low-cost adsorbents for dye removal: A review, *Bioresour. Technol.* 97 (2006) 1061–1085.
- [22] M. Ruiz, A.M. Sastre, E. Guibal, Palladium sorption on glutaraldehyde crosslinked chitosan, *React. Funct. Polym.* 45 (2000) 155–173.
- [23] W.S.W. Wan Ngah, C.S. Endud, R. Mayanar, Removal of copper(II) ions from aqueous solution onto chitosan and cross-linked chitosan beads, *React. Funct. Polym.* 50 (2002) 181–190.
- [24] N. Li, R. Bai, Development of chitosan-based granular adsorbents for enhanced and selective adsorption performance in heavy metal removal, *Water Sci. Technol.* 54 (2006) 103–113.
- [25] N.N. Thinh, P.T.B. Hanh, L.T.T. Ha, L.N. Anh, T.V. Hoang, V.D. Hoang, L.H. Dang, N.V. Khoi, T.D. Lam, Magnetic chitosan nanoparticles for removal of Cr(VI) from aqueous solution, *Mater. Sci. Eng.* 33 (2013) 1214–1218.
- [26] R.P. Pohanish, *Sittig's Handbook of Toxic and Hazardous Chemicals and Carcinogens*, William Andrew, Waltham, 2012.
- [27] Q. Yang, F. Dou, B. Liang, Q. Shen, Studies of cross-linking reaction on chitosan fiber with glyoxal, *Carbohydr. Polym.* 59 (2005) 205–210.
- [28] K.C. Gupta, F.H. Jabrail, Glutaraldehyde and glyoxal cross-linked chitosan microspheres for controlled delivery of centchroman, *Carbohydr. Res.* 341 (2006) 744–756.
- [29] H.A. Shawky, Synthesis of ion-imprinting chitosan/PVA crosslinked membrane for selective removal of Ag(I), *J. Appl. Polym. Sci.* 114 (2009) 2608–2615.
- [30] L. Martinez, F. Agnely, B. Leclerc, J. Siepmann, M. Cotte, S. Geiger, G. Couarraze, Cross-linking of chitosan and chitosan/poly(ethylene oxide) beads: A theoretical treatment, *Eur. J. Pharm. Biopharm.* 67 (2007) 339–348.
- [31] S.J. Kim, S.J. Park, S.I. Kim, Swelling behavior of interpenetrating polymer network hydrogels composed of poly(vinyl alcohol) and chitosan, *React. Funct. Polym.* 55 (2003) 53–59.
- [32] J.S. Park, J.W. Park, E. Ruckenstein, Thermal and dynamic mechanical analysis of PVA/MC blend hydrogels, *Polymer* 42 (2001) 4271–4280.
- [33] C.H. Chen, F.Y. Wang, C.F. Mao, C.H. Yang, Studies of chitosan. I. Preparation and characterization of chitosan/poly(vinyl alcohol) blend films, *J. Appl. Polym. Sci.* 105 (2007) 1086–1092.
- [34] W.S.W. Wan Ngah, A. Kamari, Y.J. Koay, Equilibrium and kinetics studies of adsorption of copper (II) on chitosan and chitosan/PVA beads, *Int. J. Biol. Macromol.* 34 (2004) 155–161.
- [35] M. Kumar, B.P. Tripathi, V.K. Shahi, Crosslinked chitosan/polyvinyl alcohol blend beads for removal and recovery of Cd(II) from wastewater, *J. Hazard. Mater.* 172 (2009) 1041–1048.
- [36] Y. Nakano, Y. Bin, M. Bando, T. Nakashima, T. Okuno, H. Kurosu, M. Matsuo, Structure and mechanical properties of chitosan/poly(vinyl alcohol) blend films, *Macromol. Symp.* 258 (2007) 63–81.
- [37] Q. Wang, Y. Du, L. Fan, Properties of chitosan/poly(vinyl alcohol) films for drug-controlled release, *J. Appl. Polym. Sci.* 96 (2005) 808–813.
- [38] D. Chen, W. Li, Y. Wu, Q. Zhu, Z. Lu, G. Du, Preparation and characterization of chitosan/montmorillonite magnetic microspheres and its application for the removal of Cr(VI), *Chem. Eng. J.* 221 (2013) 8–15.
- [39] X.J. Hu, J.S. Wang, Y.G. Liu, X. Li, G.M. Zeng, Z.L. Bao, X.X. Zeng, A.W. Chen, F. Long, Adsorption of chromium(VI) by ethylenediamine-modified cross-linked magnetic chitosan resin: Isotherms, kinetics and thermodynamics, *J. Hazard. Mater.* 185 (2011) 306–314.
- [40] Z. Zhou, S. Lin, T. Yue, T.C. Lee, Adsorption of food dyes from aqueous solution by glutaraldehyde cross-linked magnetic chitosan nanoparticles, *J. Food Eng.* 126 (2014) 133–141.
- [41] H. Yan, L. Yang, Z. Yang, H. Yang, A. Li, R. Cheng, Preparation of chitosan/poly(acrylic acid) magnetic composite microspheres and applications in the removal of copper(II) ions from aqueous solutions, *J. Hazard. Mater.* 229–230 (2012) 371–380.
- [42] D.L. Pavia, G.M. Lampman, G.S. Kriz, *Introduction to Organic Laboratory Techniques: A Microscale Approach*, fourth ed., The Thomson Corporation, California, 2007.
- [43] S.H. Pine, J.B. Hendrickson, D.J. Cram, G.S. Hammon, *Organic Chemistry*, fourth ed., McGraw-Hill, New York, NY, 1980.
- [44] K. Yao, J. Li, F. Yao, Y. Yin, *Chitosan-Based Hydrogels: Functions and Applications*, CRC Press, Florida, 2011.
- [45] Y.C. Chang, D.H. Chen, Preparation and Adsorption Properties of Monodisperse Chitosan-bound Fe₃O₄ Magnetic Nanoparticles for Removal of Cu(II) Ions, *J. Colloid Interface Sci.* 283 (2005) 446–451.
- [46] G.Y. Li, Y. Jiang, K. Huang, P. Ding, J. Chen, Preparation and properties of magnetic Fe₃O₄-chitosan nanoparticles, *J. Alloys Compd.* 466 (2008) 451–456.
- [47] J. Zhi, Y. Wang, Y. Lu, J. Ma, G. Luo, In situ preparation of magnetic chitosan/Fe₃O₄ composite nanoparticles in tiny pools of water-in-oil microemulsion, *React. Funct. Polym.* 66 (2006) 1552–1558.
- [48] B. Samiey, C.H. Cheng, J. Wu, Organic-inorganic hybrid polymers as adsorbents for removal of heavy metal ions from solutions: A review, *Materials* 7 (2014) 673–726.
- [49] B. Benguella, H. Benaissa, Cadmium removal from aqueous solutions by chitin: Kinetic and equilibrium studies, *Water Res.* 36 (2002) 2463–2474.
- [50] B.M. Weckhuysen, I.E. Wachs, R.A. Schoonheydt, Surface chemistry and spectroscopy of chromium in inorganic oxides, *Chem. Rev.* 96 (1996) 3327–3350.
- [51] G. Bayramoglu, G. Celik, M. Yilmaz, M.Y. Arica, Modification of surface properties of mycelia by physical and chemical methods: Evaluation of their Cr removal efficiencies from aqueous medium, *J. Hazard. Mater.* 119 (2005) 219–229.

- [52] F.C. Wu, R.L. Tseng, R.S. Juang, A review and experimental verification of using chitosan and its derivatives as adsorbents for selected heavy metals, *J. Environ. Manage.* 91 (2010) 798–806.
- [53] Y.C. Chang, S.W. Chang, D.H. Chen, Magnetic chitosan nanoparticles: Studies on chitosan binding and adsorption of Co(II) ions, *React. Funct. Polym.* 66 (2006) 335–341.
- [54] G. Huang, H. Zhang, J.X. Shi, T.A.G. Langrish, Adsorption of chromium(VI) from aqueous solutions using cross-linked magnetic chitosan beads, *Ind. Eng. Chem. Res.* 48 (2009) 2646–2651.
- [55] H. Zhang, Y. Tang, D. Cai, X. Liu, X. Wang, Q. Huang, Z. Yu, Hexavalent chromium removal from aqueous solution by algal bloom residue derived activated carbon: Equilibrium and kinetic studies, *J. Hazard. Mater.* 181 (2010) 801–808.
- [56] X.Z. Chu, Y.J. Zhao, Y.H. Kan, W.G. Zhang, S.Y. Zhou, Y.P. Zhou, L. Zhou, Dynamic experiments and model of hydrogen and deuterium separation with micropore molecular sieve Y at 77 K, *Chem. Eng. J.* 152 (2009) 428–433.
- [57] C. Luo, R. Wei, D. Guo, S. Zhang, S. Yan, Adsorption behavior of MnO₂ functionalized multi-walled carbon nanotubes for the removal of cadmium from aqueous solutions, *Chem. Eng. J.* 225 (2013) 406–415.
- [58] Y.C. Sharma, V. Srivastava, Comparative studies of removal of Cr(VI) and Ni(II) from aqueous solutions by magnetic nanoparticles, *J. Chem. Eng. Data* 56 (2011) 819–825.
- [59] I. Lee, C.G. Lee, J.A. Park, J.K. Kang, S.Y. Yoon, S.B. Kim, Removal of Cr(VI) from aqueous solution using alginate/polyvinyl alcohol–hematite composite, *Desalin. Water Treat.* 51 (2013) 3438–3444.
- [60] Y.J. Li, B.Y. Gao, T. Wu, D.J. Sun, X. Li, B. Wang, F.J. Lu, Hexavalent chromium removal from aqueous solution by adsorption on aluminum magnesium mixed hydroxide, *Water Res.* 43 (2009) 3067–3075.
- [61] G. Bayramoglu, M.Y. Yakuparica, Adsorption of Cr(VI) onto PEI immobilized acrylate-based magnetic beads: Isotherms, kinetics and thermodynamics study, *Chem. Eng. J.* 139 (2008) 20–28.
- [62] Y.S. Ho, Citation review of Lagergren kinetic rate equation on adsorption reactions, *Scientometrics* 59 (2004) 171–177.